

A vacuum-UV laser-induced fluorescence experiment for measurement of rotationally and vibrationally excited H_2

P. Vankan, S. B. S. Heil, S. Mazouffre, R. Engeln,^{a)} and D. C. Schram
Department of Applied Physics, Eindhoven University of Technology, P. O. Box 513, 5600 MB Eindhoven, The Netherlands

H. F. Döbele
Institut für Laser- und Plasmaphysik, Universität GH Essen, 45117 Essen, Germany

(Received 15 May 2003; accepted 6 January 2004; published 15 March 2004)

An experimental setup is built to detect spatially resolved rovibrationally excited hydrogen molecules via laser-induced fluorescence. To excite the hydrogen molecules, laser radiation is produced in the vacuum UV part of the spectrum. The laser radiation is tunable between 120 nm and 230 nm and has a bandwidth of 0.15 cm^{-1} . The wavelength of the laser radiation is calibrated by simultaneous recording of the two-photon laser induced fluorescence spectrum of nitric oxide. The excited hydrogen populations are calibrated on the basis of coherent anti-Stokes Raman scattering measurements. A population distribution is measured in the shock region of a pure hydrogen plasma expansion. The higher rotational levels ($J > 5$) show overpopulation compared to a Boltzmann distribution determined from the lower rotational levels ($J \leq 5$). © 2004 American Institute of Physics. [DOI: 10.1063/1.1688435]

I. INTRODUCTION

Rovibrationally excited hydrogen molecules ($H_2^{r,v}$) can influence the hydrogen kinetics in plasmas to a large extent. Molecular reactions that involve rovibrationally excited molecules can be much more efficient compared to reactions with ground-state molecules. This increased reactivity is caused by the extra energy stored in rotation and vibration. The production of the hydrogen negative ion (H^-) via dissociative attachment, for example, becomes five orders of magnitude more efficient when the vibration of the hydrogen molecule is increased from $v=0$ to $v=5$.¹ Another example of the increased reactivity of rovibrationally excited molecules is the charge exchange of H^+ with H_2 . This process becomes resonant for $v=4$, which increases the cross section by several orders.²

To understand the influence of $H_2^{r,v}$ in plasmas, it is vital to have information on the density distribution over the various levels. High rotational levels of molecular hydrogen ($J > 5$) are generally found to be overpopulated compared to a Boltzmann (i.e., a thermal) distribution. High vibrational levels have also been found to be overpopulated.³ These rotational and vibrational overpopulations are related to the creation processes of the $H_2^{r,v}$.

In low-temperature plasmas, the main creation processes for $H_2^{r,v}$ are the direct and indirect electron excitation processes.^{4,5} In those cases, the nonthermal distributions are believed to be caused by the high-energy tail of the electron energy distribution function. These creation processes depend critically on the electron density and on the electron energy distribution function. However, in environments

where the electron density and electron energy are low, the electron excitation processes are very inefficient. In such environments, surfaces may influence the vibrational and rotational excitation to a large extent. On a surface, molecular hydrogen ions⁶ as well as atomic hydrogen radicals^{7,8} can recombine, forming rovibrationally excited H_2 . Hall *et al.*⁸ and Eenshuistra *et al.*,⁷ for example, measured vibrational overpopulations near heated filaments, where the electron density was very low. The overpopulated density distribution was explained by surface recombination of hydrogen atoms into high vibrationally excited hydrogen molecules.

Measuring the population distribution over the rotational and vibrational levels of the electronic ground state necessitates state selective and often spatially resolved measurements. Such measurements are commonly performed using laser spectroscopy. In the case of H_2 , however, laser spectroscopy is not straightforward, since purely rovibrational transitions are not allowed and the energy gap to the first electronically excited state ($B^1\Sigma_u^+$) is large ($\sim 11 \text{ eV}$). A possible technique to measure the density of the lower vibrational levels is coherent anti-Stokes Raman scattering (CARS).⁹ However, for higher vibrational levels ($v \geq 2$), the CARS technique has serious limitations. In order to probe the higher vibrational levels, laser-induced fluorescence (LIF) with excitation to the $B^1\Sigma_u^+$ state can be used. To excite to this state, radiation is needed with a wavelength below 165 nm, the vacuum-UV region (VUV). This VUV radiation can be produced using the stimulated anti-Stokes Raman scattering (SARS) process.¹⁰

In this article, we present an experimental setup which can measure $H_2^{r,v}$ from $v=2$ to $v=13$, i.e., with wavelengths between 120 and 165 nm. The setup will be described in detail. Some spectra and a rovibrational distribution will be

^{a)}Author to whom correspondence should be addressed; electronic mail: r.engeln@phys.tue.nl

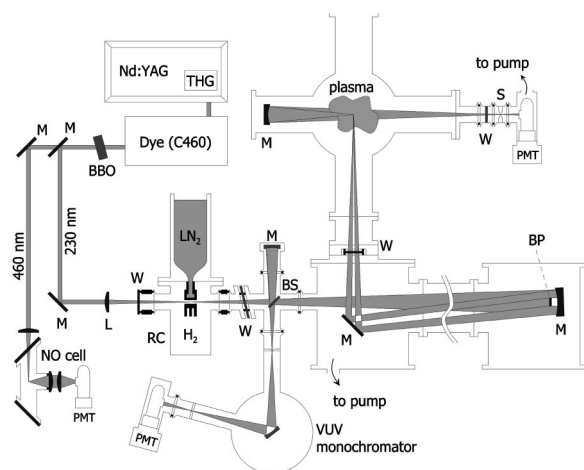


FIG. 1. The experimental arrangement. M stands for mirror, L is the quartz lens, RC is the Raman cell, W is a window, S is a slit, BS is the beam splitter, and BP the blocking plate.

presented and the density calibration via CARS will be discussed.

II. EXPERIMENTAL SETUP

As a hydrogen source, a cascaded arc is used. The cascaded arc and the vacuum chamber to which the arc is connected, are extensively described elsewhere.¹¹ In short, the arc produces a subatmospheric, partially ionized, and partially dissociated plasma. The power input is typically 2–10 kW. The plasma expands supersonically into the vacuum chamber, at typical pressures of 10–200 Pa. The expanding plasma jet collides with the background gas in the vacuum chamber forming a shock structure.^{12,13} Behind the shock, the plasma jet is subsonic. The plasma source can be moved parallel to the expansion axis as well as perpendicular to the expansion axis. This enables spatially resolved measurements throughout the complete expansion structure. Furthermore, a temperature controlled substrate can move perpendicular and parallel to the expansion axis, enabling spatially resolved measurements in front of the surface.

A scheme of the experimental arrangement is shown in Fig. 1. A frequency doubled Nd:YAG laser (GCR230, Spectra Physics, Germany) operated at 20 Hz is used to pump a tunable dye laser (Precisionscan, Sirah, Germany), producing light between 430 and 470 nm. This light is frequency doubled in a Beta Barium Borate crystal resulting in 5 ns pulses of 5–10 mJ, with a bandwidth of 0.15 cm^{-1} .

After separation of the dye laser fundamental beam using three dielectric mirrors, the light is focused into a Raman cell using a 19 cm focal distance quartz lens. The details of the Raman cell design and the principles of anti-Stokes (AS) generation are described elsewhere.^{10,14} In short, the Raman cell is filled with hydrogen at a pressure around 120 kPa. A copper finger in the center of the cell is cooled with liquid nitrogen. The laser is now focused into a cylindrical hole in the cold finger. At the laser focus, the high-power density enables the SRS process. In this process, a set of laserlike coherent beams, the so-called Stokes (S) and AS beams, is generated. Every subsequent AS order is shifted up

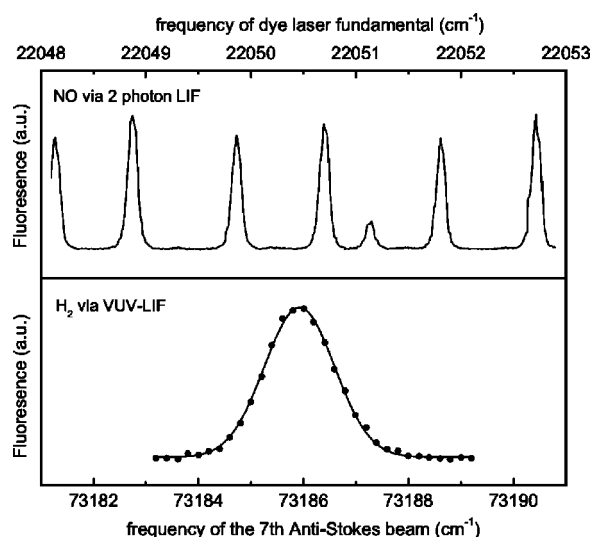


FIG. 2. Two-photon LIF spectrum of the NO γ band together with a transition of the Lyman band of H_2 [$X(v=4, J=7) \rightarrow B(v=0, J=6)$]. The relative fluorescence is plotted in arbitrary units (a.u.). The dots in the lower part are data points and the line is a Gaussian fit to the data points.

in frequency by the vibrational Raman shift of H_2 , i.e., 4155.22 cm^{-1} . Tunable, narrowband, laserlike radiation can now be produced covering the complete VUV region from 230 nm down to 120 nm. This coherent laserlike radiation exhibits most of the laser properties but is not real laser radiation. For convenience, it will still be referred to as laser radiation. The radiation is used to excite the hydrogen molecules from a rovibrational state in the electronic ground state via one of the Lyman transitions $X^1\Sigma_g^+ \rightarrow B^1\Sigma_u^+$ to the first electronically excited state.¹⁵ This state then radiatively decays back to the ground state. The fluorescence generated in this LIF process is detected, giving information on density and temperature of the lower level.

In order to know the wavelength accurately, the remnant dye laser fundamental beam is used to excite nitric oxide (NO) in a cell via a two-photon transition of the γ band. The fluorescence back to the NO ground state is imaged onto a photomultiplier tube (PMT) (R7154, Hamamatsu, Japan). The recorded spectrum, which is well known from literature,¹⁶ is used to calibrate the wavelength of the dye laser. In a typical measurement, the excitation spectrum of the hydrogen molecules in the plasma and the NO in the gas cell can be recorded simultaneously as shown in Fig. 2, where the laser is scanned over the H_2 line [$X(v=4, J=7) \rightarrow B(v=0, J=6)$].

All Raman orders, S and AS, together with the depleted pump beam leave the Raman cell simultaneously. The laser beams are focused using a concave VUV mirror and then directed into the vacuum chamber using a flat VUV mirror. In order to reduce the stray light (which is mainly caused by the depleted pump beam), a metal disk can be placed at the center of the concave VUV mirror. Since the spatial beam profiles of the S and pump beams are close to Gaussian, whereas the profiles of the AS beams are concentric rings, the disk can block the relatively high power pump beam and S beams, reducing the stray light. A thin MgF_2 plate, located just after the Raman cell, reflects a small part of the laser

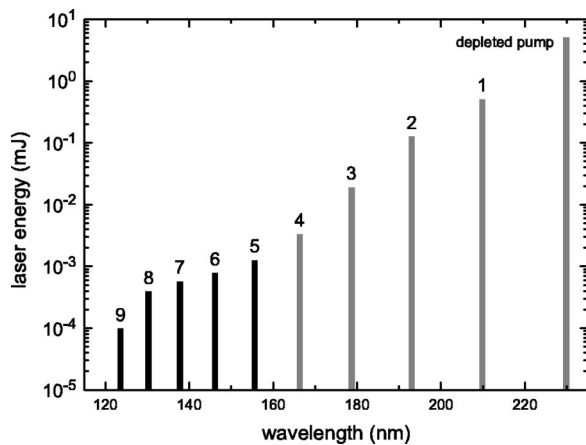


FIG. 3. The AS energy as a function of wavelength. The pressure in the Raman cell was 150 kPa and the laser energy was 7.5 mJ per pulse.

light onto a concave mirror which focuses the light onto the entrance slit of a 50 cm VUV monochromator (McPherson). A solar blind PMT (R7639, Hamamatsu, Japan) monitors the intensity of the AS, that is used for the excitation. In Fig. 3, the relative AS intensity is plotted as function of the wavelength. This measurement was done at a H_2 pressure in the Raman cell of 150 kPa and a laser energy of about 8 mJ per shot. The intensities plotted in Fig. 3 have been corrected for the wavelength dependence of the detection efficiency. Since the VUV radiation is efficiently absorbed by oxygen, the complete optical system behind the Raman cell (reference branch, AS focusing and detection branch) is operated under a vacuum at a pressure of about 1 mPa.

The fluorescence is detected perpendicular to the laser beam. A concave VUV mirror focuses the fluorescence through a slit mask. The detection volume is defined by the waist of the focus ($\sim 200 \mu\text{m}$) and by the rectangular slit mask ($1.0 \times 0.5 \text{ mm}^2$). The fluorescence is detected by a solar blind PMT (R1259, Hamamatsu, Japan). The PMT can be gated to protect it from plasma radiation. Both the reference and the fluorescence signal are recorded shot-to-shot by an oscilloscope (LT372, LeCroy, France). The fluorescence is recorded as a function of the excitation wavelength in typically 50 steps. At every wavelength, typically 100 shots are recorded. Since the number of fluorescence photons can be relatively small (in the order of 100 photons/shot), the fluorescence is averaged prior to the correction for laser intensity. For this correction, the averaged fluorescence signal is divided by the average reference signal, i.e., the relative laser intensity. From the area under the fluorescence peaks, the density can be calculated, and from the width of the mainly Doppler broadened peaks, the temperature can be determined.^{17,18}

III. RESULTS AND DISCUSSION

To illustrate the working of the setup, part of the Lyman band spectrum has been recorded, as can be seen in Fig. 4. Here, the fluorescence is plotted as a function of the pump beam wavelength, i.e., the second harmonic (SH) of the dye laser. When the dye laser, and thus its SH, is scanned, all the AS beams are also scanned. The fluorescence from the vari-

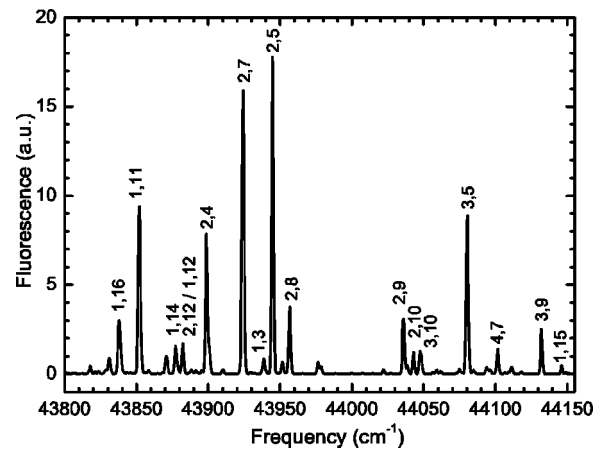


FIG. 4. Part of the H_2 Lyman spectrum. The different frequency scales belonging to the different excitation AS beams were converted into one frequency scale, that of the SH of the dye laser, which is the horizontal axis. This is called multiplexing. The rovibrational excitation of the lower level of the transitions, depicted with (v, J) , is shown near the corresponding peaks.

ous transitions in the spectrum can be induced by different AS orders, belonging to different wavelengths. The wavelength, or energy, scale of the spectrum is therefore the addition of all the energy scales of all the AS beams used for the excitation. This is called multiplexed LIF (*m*-LIF). The wavelength calibration was necessary in order to identify the peaks in the spectrum and their corresponding excitation AS beam.

When recording transitions from different lower levels, one can measure the population distribution. Such a population distribution has been plotted in Fig. 5. The density divided by the degeneracy is plotted as function of the energy of the corresponding state. The degeneracy is given by $(2J+1)(2N+1)$, where J is the quantum number of the angular momentum and N the quantum number of the nuclear spin; in the case of H_2 , $N=0$ for even J and $N=1$ for odd J . To arrive at correct relative densities, the measurements have been corrected for the excitation efficiency (Ein-

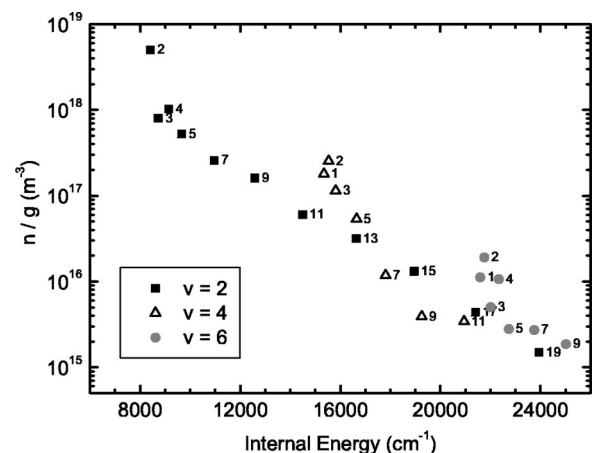


FIG. 5. Number density per statistical weight of H_2 , in the $v=2, 4$, and 6 vibrational states as a function of the internal rovibrational energy. The numbers near the symbols denote the corresponding rotational levels. This population distribution was measured in the shock region of a pure hydrogen plasma expansion. The densities have been calibrated using previous CARS measurements.

stein coefficient, laser energy, and transmission through the optics in the excitation branch are taken into account) and for the wavelength dependent detection efficiency (window transmission, mirror reflectivity, and quantum efficiency of the PMT). The latter three have been individually measured by the manufacturer. The relative LIF densities have been calibrated using previous CARS measurements.⁹ Those show overlap with the presented *m*-LIF measurements at the H₂(*X*) (*v*=2, *J*=3) state. Using the *m*-LIF technique with the present setup, densities down to 10¹⁵ m⁻³ can be detected.

From the lower rotational levels, a rotational temperature can be determined assuming a Boltzmann distribution. This temperature is about 900 K and is approximately equal to the temperature determined from the width of the fluorescence lines. This indicates that the lower rotational levels are consistent with thermal equilibrium.

However, both the CARS⁹ and the *m*-LIF measurements show overpopulation of the higher rotational levels (*J*>5) compared to the Boltzmann distribution determined from the lower levels. For example, in the *v*=6 state, the population in the rotational levels *J*=7 and *J*=9 is clearly higher than described by a Boltzmann distribution determined from populations in *J*=1 to *J*=5. In the state *v*=2, rotational levels have even been observed up to *J*=19. The temperature that would result from these higher levels is approximately 3600 K, which is in the same order of magnitude of the apparent vibrational temperature of about 3000 K. Since this vibrational temperature is much higher than the translational temperature, it can be concluded that the higher rotational levels are not consistent with thermal equilibrium. In the present situation, this is still to be explained since the local electron temperature is much lower. It can be an effect of redistribution of rovibrational excitation, created in wall association. Also, the residual excitation created in the plasma source could contribute. The measured distribution is

probably a combination of both effects. To better understand the departure from the Boltzmann distribution, further work is needed.

ACKNOWLEDGMENTS

This work is part of the research program of the Dutch Foundation for Fundamental Research on Matter (FOM). The work is also supported by the Euratom Foundation. The authors greatly appreciate the skillful technical assistance of M. J. F. van de Sande, J. F. C. Jansen, A. B. M. Hüsken, and H. M. M. de Jong.

- ¹A. Peet Hickman, *Phys. Rev. A* **43**, 3495 (1991).
- ²P. S. Krstić, D. R. Schultz, and R. K. Janev, *Phys. Scr.*, T **96**, 61 (2002).
- ³T. Mosbach, H.-M. Katsch, and H. F. Döbele, *Phys. Rev. Lett.* **85**, 3420 (2000).
- ⁴R. Celiberto, R. K. Janev, A. Laricchiuta, M. Capitelli, J. M. Wadehra, and D. E. Atems, *At. Data Nucl. Data Tables* **77**, 161 (2001).
- ⁵J. R. Hiskes, *J. Appl. Phys.* **70**, 3409 (1991).
- ⁶J. R. Hiskes and A. M. Karo, *J. Appl. Phys.* **67**, 6621 (1990).
- ⁷P. J. Eenshuistra, J. H. M. Bonnie, J. Los, and H. J. Hopman, *Phys. Rev. Lett.* **60**, 341 (1988).
- ⁸R. I. Hall, I. Čadež, M. Landau, F. Pichou, and C. Schermann, *Phys. Rev. Lett.* **60**, 337 (1988).
- ⁹R. Meulenbroeks, R. A. H. Engeln, J. A. M. van der Mullen, and D. C. Schram, *Phys. Rev. E* **53**, 5207 (1996).
- ¹⁰H. F. Döbele, *Plasma Sources Sci. Technol.* **4**, 224 (1995).
- ¹¹M. C. M. van de Sande, J. M. de Regt, G. M. Janssen, J. A. M. van der Mullen, D. C. Schram, and B. van der Sijde, *Rev. Sci. Instrum.* **63**, 3369 (1992).
- ¹²S. Mazouffre, M. G. H. Boogaarts, J. A. M. van der Mullen, and D. C. Schram, *Phys. Rev. Lett.* **84**, 2622 (2000).
- ¹³S. Mazouffre, P. Vankan, R. Engeln, and D. C. Schram, *Phys. Plasmas* **8**, 3824 (2001).
- ¹⁴M. Spaan, A. Goehlich, V. Schulz-von der Gathen, and H. F. Döbele, *Appl. Opt.* **33**, 3865 (1994).
- ¹⁵H. Abgrall, E. Roueff, F. Launay, J.-Y. Roncin, and J.-L. Subtil, *Astron. Astrophys., Suppl. Ser.* **101**, 273 (1993).
- ¹⁶P. H. Paul, *J. Quant. Spectrosc. Radiat. Transf.* **57**, 581 (1997).
- ¹⁷W. Demotröder, *Laser Spectroscopy* (Springer, Berlin, 1988).
- ¹⁸M. G. H. Boogaarts, S. Mazouffre, H. W. P. van der Heijden, G. J. Brinkman, P. Vankan, J. A. M. van der Mullen, D. C. Schram, and H. F. Döbele, *Rev. Sci. Instrum.* **73**, 73 (2002).